

THE BIGGEST EXPLOSIONS IN THE UNIVERSE

JARRETT L. JOHNSON¹, DANIEL J. WHALEN^{1,2}, WESLEY EVEN³, CHRIS L. FRYER³,
ALEX HEGER⁴, JOSEPH SMIDT¹ AND KE-JUNG CHEN⁵

¹Nuclear and Particle Physics, Astrophysics and Cosmology Group (T-2),
Thermonuclear Applications Physics Group (XTD-6),
Los Alamos National Laboratory, Los Alamos, NM 87545; jlj@lanl.gov

²Universität Heidelberg, Zentrum für Astronomie, Institut für Theoretische Astrophysik,
Albert-Ueberle-Str. 2, 69120 Heidelberg, Germany

³Computational Physics and Methods Group (CCS-2),
Los Alamos National Laboratory, Los Alamos, NM 87545

⁴Monash Centre for Astrophysics, Monash University, Victoria, 3800, Australia and

⁵School of Physics and Astronomy, University of Minnesota, Minneapolis, MN 55455

Draft version August 2, 2013

ABSTRACT

Supermassive primordial stars are expected to form in a small fraction of massive protogalaxies in the early universe, and are generally conceived of as the progenitors of the seeds of supermassive black holes (BHs). Supermassive stars with masses of $\sim 55,000 M_{\odot}$, however, have been found to explode and completely disrupt in a supernova (SN) with an energy of up to $\sim 10^{55}$ erg instead of collapsing to a BH. Such events, $\sim 10,000$ times more energetic than typical SNe today, would be among the biggest explosions in the history of the universe. Here we present a simulation of such a SN in two stages. Using the RAGE radiation hydrodynamics code we first evolve the explosion from an early stage through the breakout of the shock from the surface of the star until the blast wave has propagated out to several parsecs from the explosion site, which lies deep within an atomic cooling dark matter (DM) halo at $z \simeq 15$. Then, using the GADGET cosmological hydrodynamics code we evolve the explosion out to several kiloparsecs from the explosion site, far into the low-density intergalactic medium. The host DM halo, with a total mass of $4 \times 10^7 M_{\odot}$, much more massive than typical primordial star-forming halos, is completely evacuated of high density gas after $\lesssim 10$ Myr, although dense metal-enriched gas recollapses into the halo, where it will likely form second-generation stars with metallicities of $\simeq 0.05 Z_{\odot}$ after $\gtrsim 70$ Myr. The chemical signature of supermassive star explosions may be found in such long-lived second-generation stars today.

Subject headings: Cosmology: theory — early universe — supernovae: general

1. INTRODUCTION

Recently, there has been renewed interest in the long-standing theoretical possibility that supermassive stars (SMSs), with masses of 10^4 – $10^6 M_{\odot}$ inhabited the early universe (see e.g., Volonteri 2012) and their possible fates (e.g., Iben 1963; Fowler & Hoyle 1964; Appenzeller & Fricke 1972; Shapiro & Teukolsky 1979; Bond et al. 1984; Fuller et al. 1986).

One of the main motivations for their study comes from observations of quasars at $z \simeq 6$ – 7 which are inferred to be powered by black holes (BHs) with masses exceeding $10^9 M_{\odot}$ (e.g., Willott et al. 2003; Fan et al. 2006; Mortlock et al. 2011). Given the short time (< 800 Myr) available for such massive BHs to grow via accretion from their initial ‘seed’ masses, as derived from the most recent cosmological parameters inferred by e.g., the *Wilkinson Microwave Anisotropy Probe* (Komatsu et al. 2011),¹ and the suppression of BH growth due to the strong radiative feedback from both stars (e.g., Whalen et al. 2004; Wise & Abel 2007; O’Shea & Norman 2008) and the BHs themselves (e.g., Pelupessy et al. 2007; Alvarez et al. 2009; Milosavljević et al. 2009; Jeon et al. 2012; Park & Ricotti 2012), it now appears more likely than ever

that the seeds of the most massive early BHs must have been quite massive themselves (e.g., $\gtrsim 10^5 M_{\odot}$; see Johnson et al. 2012a; also e.g., Shapiro 2005; Volonteri & Rees 2006; Natarajan & Volonteri 2012). Whereas the majority of the first, Population (Pop) III stars may have had masses of ~ 20 – $500 M_{\odot}$ (e.g., Abel et al. 2002; Bromm & Larson 2004; Yoshida et al. 2008; Greif et al. 2011), the best candidates for the seeds of SMBHs are thus much more massive (and rare) supermassive primordial stars.

An additional, and independent, reason to consider SMSs in the early universe is that the conditions required for their formation are now thought to be realized much more often than was previously assumed. The most widely discussed avenue for the formation of SMSs is via the direct gravitational collapse of hot ($\simeq 10^4$ K) primordial gas in so-called atomic cooling dark matter (DM) halos at $z \gtrsim 10$ (e.g., Bromm & Loeb 2003; Begelman et al. 2006; Lodato & Natarajan 2006; Spaans & Silk 2006; Regan & Haehnelt 2009; Choi et al. 2013; Latif et al. 2013a,b).² In this scenario, the gas in the protogalaxy remains at the virial temperature of $\sim 10^4$ K because H_2 molecules have been photodissociated by the Lyman-Werner (LW) background, leading to the rapid formation of SMSs via the accretion of gas at rates $\sim 10^2$ – 10^3 times

¹ Adopting the cosmological parameters reported recently by the *Planck* Collaboration (2013) yields a similar time available for seed growth.

² We note that other formation mechanisms stemming from shocks (Inayoshi et al. 2012) and magnetic fields (Sethi et al. 2010) have also been suggested.

higher than in the formation of most Pop III stars from H_2 -cooled gas. The flux of radiation required to keep the gas H_2 -free depends on its spectrum, with lower fluxes required if it is produced by metal-enriched stars instead of Pop III stars (e.g., Shang et al. 2010). Recent work by independent groups has shown that Pop II star-forming galaxies in the early universe are able to produce sufficient H_2 -dissociating radiation to prevent the cooling of primordial gas in a substantial fraction of atomic cooling halos, thereby leading to the seeding of these halos with SMSs that can collapse into BHs (see Dijkstra et al. 2008; Agarwal et al. 2012; Petri et al. 2012; Johnson et al. 2013). Indeed, Agarwal et al. (2012, 2013) find that a large fraction of the SMBHs in the centers of galaxies today may have been seeded by SMSs. Strengthening these conclusions are other recent results which suggest that lower LW fluxes may be required for the formation of SMSs, due to a reduced role of H_2 self-shielding (Wolcott-Green et al. 2011) and the presence of significant turbulence or magnetic fields (Van Borm & Spaans 2013).

Complementary studies have been undertaken to understand the growth and evolution of SMSs, as well. Modeling the growth of accreting protostars with masses up to $\simeq 10^3 M_\odot$, Hosokawa et al. (2012) have shown that they emit little high energy radiation that could halt their continued accretion, and Inayoshi et al. (2013) have shown that pulsational instabilities are likewise unable to halt their growth. Johnson et al. (2012b) modeled the growth of SMSs to much higher masses and showed that, even if they are able to emit the copious ionizing radiation characteristic of main sequence Pop III stars, which may occur once the accretion rate becomes sufficiently low (Schleicher et al. 2013), radiative feedback is not able to stop their growth up to at least $\sim 10^5 M_\odot$. At the highest accretion rates expected for these objects ($\gtrsim 1 M_\odot \text{ yr}^{-1}$; Wise et al. 2008; Shang et al. 2010; Johnson et al. 2011), the masses of primordial SMSs are only limited by the $\lesssim 4 \text{ Myr}$ that they have to accrete gas before they collapse to BHs (Begelman 2010).

Whereas the majority of SMSs are expected to collapse to black holes with little or no associated explosion (e.g., Fryer & Heger 2011; see also Fuller & Shi 1998; Linke et al. 2001), it is possible that some fraction instead explode as extremely energetic supernovae (SNe; e.g., Fuller et al. 1986; Montero et al. 2012; Whalen et al. 2012a, 2013d). In particular, Heger et al. (2013) have found from stellar evolution calculations including post-Newtonian corrections to gravity that SMSs with masses in a narrow range around $\simeq 55,000 M_\odot$ end their lives as extraordinarily luminous SNe.³ With energies of almost 10^{55} erg , these thermonuclear explosions are among the most energetic in the history of the universe.

Here we expand on the radiation hydrodynamics simulations presented by Whalen et al. (2012a) and simulate the long-term evolution of a SMS SN in its cosmological environment, in order to show how these gargantuan explosions impact both the formation of the first galaxies and the chemical signature of the first stars. In the

³ These SNe would appear much brighter than other types of Pop III SNe (e.g., Scannapieco et al. 2005; Hummel et al. 2012; Pan et al. 2012; Tanaka et al. 2012, 2013; Whalen et al. 2012b, 2013a,b,c; de Souza et al. 2013).

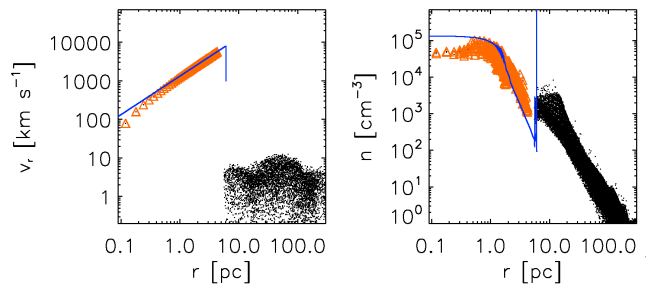


FIG. 1.— The initial conditions for the GADGET 3-D cosmological simulation. The blue curves show the radial velocity (*left*) and hydrogen number density (*right*) profiles resulting from the 1-D RAGE simulation of the early evolution of the SMS SN remnant, up to the time when the shock extends out to 6 pc from the explosion site. The orange triangles denote the GADGET SPH particles representing the SN ejecta that are fit to the RAGE output. The black points denote the SPH particles within the cosmological halo hosting the explosion.

next section, we describe the multi-scale simulations that we have carried out to model the evolution of the explosion from its breakout from the surface of the star to the propagation of the blast wave into the intergalactic medium (IGM). In Section 3, we present our results on the energetics and dynamics of the explosion, as well as on metal enrichment and second-generation star formation. In Section 4, we conclude with a brief discussion of our results.

2. SIMULATION SETUP

Here we describe the two simulations that we have carried out. The first is a 1-D radiation hydrodynamics calculation using the Los Alamos National Laboratory RAGE code (Gittings et al. 2008) which allows to track the propagation of the SN blast wave out to several parsecs from the explosion site, deep within the host atomic cooling halo. For the second, we map the results of the first into a 3-D cosmological simulation using the GADGET hydrodynamics code (Springel et al. 2001; Springel & Hernquist 2002). Our use of these two simulation codes for the phases of the SN in which they are most well-suited to accurately model the explosion, from small (AU) scales to large (kpc) scales, constitutes a significant improvement over previous cosmological simulations of SN feedback.

2.1. Stellar and Early Supernova Evolution

For the SMS progenitor of the SN we adopt the $55,000 M_\odot$ stellar model described in Whalen et al. (2012a), which was evolved until the onset of explosion, using the *Kepler* code (Weaver et al. 1978; Woosley et al. 2002). The explosion was then followed using *Kepler* and was confirmed (Chen et al., 2013) using the CASTRO code (Almgren et al. 2010). The explosion completely disrupts the star and yields an explosion energy of $7.7 \times 10^{54} \text{ erg}$ (Heger et al. 2013). The RAGE code is then used to simulate the SN from the breakout of the shock from the surface of the star until the blast wave has propagated through a circumstellar medium with a density $\geq 10^2 \text{ cm}^{-3}$ (and a density profile $\propto r^{-2}$) out to several parsecs from the explosion site. Up to this point, the stellar evolution calculation and the simulation of

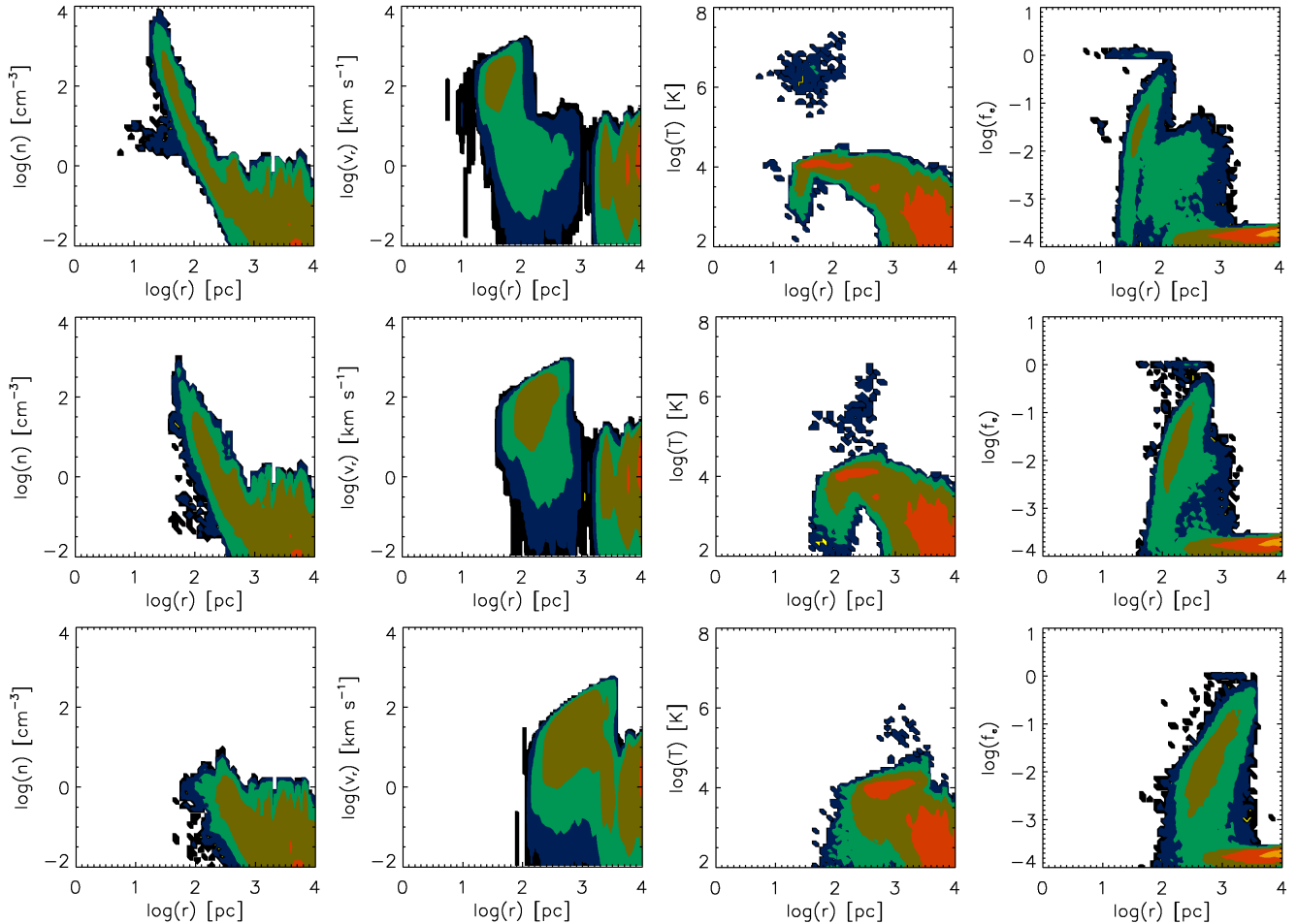


FIG. 2.— Properties of the gas in the vicinity of the SN at 100 kyr (*top panels*), 1 Myr (*middle panels*) and 10 Myr (*bottom panels*) after the explosion of the central SMS. From left to right, as functions of the distance from the explosion site, are the number density of hydrogen nuclei, outward radial velocity, gas temperature and free electron fraction. Contours denote the distribution of the gas, with the mass fraction varying by an order of magnitude across contour lines. The $\sim 1000 \text{ km s}^{-1}$ shock completely disperses the dense ($n > 10 \text{ cm}^{-3}$) gas in the center of the host atomic cooling halo, but is only slightly decelerated even after propagating well beyond the $\sim 1 \text{ kpc}$ virial radius of the halo.

the early phases of the SN are the same as described in Whalen et al. (2012a), to which we refer the reader for more detailed discussion of the calculations (see also Frey et al. 2013).

The blue curves in Figure 1 show the velocity (left panel) and density (right panel) profiles of the SN ejecta at the end of the RAGE simulation, at which point the shock has propagated out to 6 pc from the explosion site. The $55,000 M_{\odot}$ of ejecta, $23,000 M_{\odot}$ of which is heavy elements produced during the evolution and explosion of the progenitor, are traveling at almost $10,000 \text{ km s}^{-1}$ outward from the center of the host atomic cooling halo. It is from this point that we map these velocity and density profiles into a self-consistently evolved atomic cooling halo in a much larger cosmological volume.

2.2. Cosmological Blast Wave

To simulate the subsequent evolution of the SN blast wave in the appropriate cosmological environment, we map the velocity and density profiles obtained from the smaller-scale RAGE simulation into the center of a $4 \times 10^7 M_{\odot}$ atomic cooling DM halo, the type of which

is expected to host the formation of SMSs in the early universe. The halo is identified in a 1 Mpc^3 (comoving) cosmological volume which has been evolved from $z = 100$ down to $z \simeq 15$ under the influence of a uniform, elevated H_2 -dissociating (Lyman-Werner; LW) radiation field, which prevents the gas from cooling and is assumed to lead to formation of a single SMS. Further details of the cosmological simulation up to this point are described in Johnson et al. (2011), who considered the impact of the alternative end state of such a SMS, a rapidly accreting BH.

To map the output of the (Eulerian) RAGE simulation into the (Lagrangian) smoothed particle hydrodynamics (SPH) GADGET simulation, we assigned the central 460 SPH particles, constituting the $55,000 M_{\odot}$ of gas within $\simeq 6 \text{ pc}$ of the densest particle in the halo, outward (radial) velocities and hydrogen number densities so as to match those from the RAGE simulation. The fits that we obtain are shown in Fig. 1, with the inner $55,000 M_{\odot}$ in SPH particles constituting the ejecta denoted by orange triangles and the unperturbed particles residing in the outskirts of the halo denoted by black circles. Whereas we fit

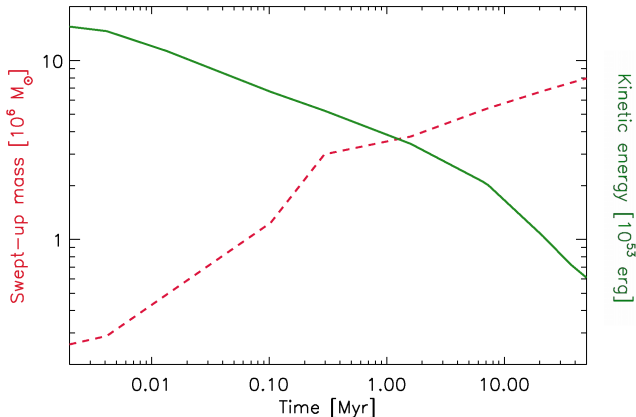


FIG. 3.— The mass of material swept up by the shock (*red dashed line*) and the total kinetic energy of the swept-up material (*green solid line*), as a function of time since the SN. The majority of the kinetic energy is radiated away within the first 10^4 yr, and after 50 Myr all but $\sim 1\%$ has been lost. The majority of the material that is overtaken by the shock is swept-up after 1 Myr, with the total swept-up mass approaching $10^7 M_{\odot}$.

the velocity profile very well, due to the mapping from an Eulerian to Lagrangian code the density profile is somewhat noisier.⁴ Nonetheless, the basic features of the density profile containing the vast majority of the mass are represented, and the overall energy and momentum are also well-matched. From the initial conditions shown in Fig. 1 we restart the cosmological SPH simulation, the results of which we present in the next section.

Beyond mapping into it the blast profile of the SMS SN, we have chosen to leave the gas in the host halo otherwise unchanged. We have made this simplifying choice, in light of the large uncertainties in the radiative output of rapidly accreting SMSs, due to which it is unclear how the radiation emitted during the brief (~ 2 Myr) lifetime of the star will impact the medium within the host halo. Even if the star emits copious ionizing radiation, as main sequence Pop III stars are expected to do, it may be that the H II region created by the star is confined to the innermost regions of the halo (Johnson et al. 2012; see also Hosokawa et al. 2012 on the possibility of even less energetic radiation being emitted during the protostellar phase). It is possible, on the other hand, that ionizing radiation is able to escape out into the halo, if the accretion flow is highly anisotropic (e.g., McKee & Tan 2008), or if accretion is intermittent (e.g., Clark et al. 2011; Smith et al. 2011; Vorobyov et al. 2013), in which case radiation could break out during periods of reduced accretion.

Whereas the small-scale structure of the interstellar gas in the simulation we present here is subject to the limited resolution of the cosmological simulation into which we place the expanding blast wave, we note that at sub-resolution scales ($\lesssim 1$ pc) it is possible that a substantial amount of energy in the explosion is radiated

⁴ Note in Fig. 1 that the density spike at the shock front in the RAGE output contains less mass than is contained in a single GADGET SPH particle, and so there are no particles representing this particular parcel of gas in the cosmological simulation. This illustrates the fundamental difficulty in matching output from an Eulerian, adaptive mesh refinement code to an SPH code.

away (e.g., Kitayama & Yoshida 2005; Whalen et al. 2008; de Souza et al. 2011; Vasiliev et al. 2012). We shall address how such additional radiative losses would affect the dynamics of the blast wave and the metal enrichment of the host halo and IGM in future work.

3. RESULTS

Here we present the results of our cosmological hydrodynamics simulation, with particular attention paid to the dynamics of the expanding blast wave and to the enrichment of the IGM by the metal-rich SN ejecta.

3.1. Dynamics and Energetics

The injection of almost 10^{55} erg at a single explosion site has a dramatic impact on the host halo. Figure 2 shows the properties of the gas in the vicinity of the halo, as a function of the distance from the explosion site at its center. As the left-most panels show, the blast results in the complete evacuation of high-density ($n \gtrsim 10 \text{ cm}^{-3}$) gas within 10 Myr, with the material overtaken by the shock being carried out beyond the virial radius of the halo (at $r \simeq 10^3$ pc) at up to $\simeq 10^3 \text{ km s}^{-1}$. This material is also shock heated to temperatures up to $\sim 10^8$ K, resulting in its almost complete ionization, as shown in the right-panels. The gas, however, rapidly cools due to inverse Compton scattering of CMB photons, H and He atomic line emission, and bremsstrahlung, as also found (using the same GADGET code) in the less-energetic (10^{52} erg) pair instability supernova (PSN) explosion in a $2.5 \times 10^5 M_{\odot}$ DM halo simulated by Greif et al. (2007), as well as in the 1-D calculation of a very energetic (10^{54} erg) Pop III SN in a slightly less massive ($10^7 M_{\odot}$) DM halo presented in Kitayama & Yoshida (2005).

As shown in Figure 3, most ($\simeq 90\%$) of the 7.7×10^{54} erg initially in the blast is radiated away via these processes within 10^4 yr. Nevertheless, the momentum of the blast is conserved and the shock continues to propagate into the IGM, sweeping up the majority of the mass after $\simeq 1$ Myr. By 50 Myr, at which time $\simeq 99\%$ of the energy has been radiated away, the shock has propagated out to $\simeq 5\text{--}10$ kpc and has swept up almost $10^7 M_{\odot}$.

Figure 4 shows the properties of the gas in the vicinity of the explosion site within a 400 pc (comoving) slice of the cosmological volume, at 1 Myr, 10 Myr and 50 Myr after the explosion of the SMS. Comparing the radial velocity field (second column from the left) to the cosmological density field (far left column), it is clear that the blast wave propagates most rapidly into the low-density voids while its progress is halted in the direction of the high-density filaments, at the intersection of which lies the host halo. Figs. 2 and 4 also show the same general trend that, at late times, the most strongly shock-heated and highest-velocity material is located behind the shock front several kpc from the explosion site. The cooler material within the ($\simeq 1$ kpc) virial radius of the host halo is able to begin recollapsing after 50 Myr. As we discuss next, this gas is likely to form second-generation stars that are enriched to fairly high metallicities.

3.2. Metal Enrichment and Second-Generation Star Formation

As is also expected for less energetic PSNe from Pop III stars with masses of $\sim 200 M_{\odot}$ (e.g., Heger et al. 2003),

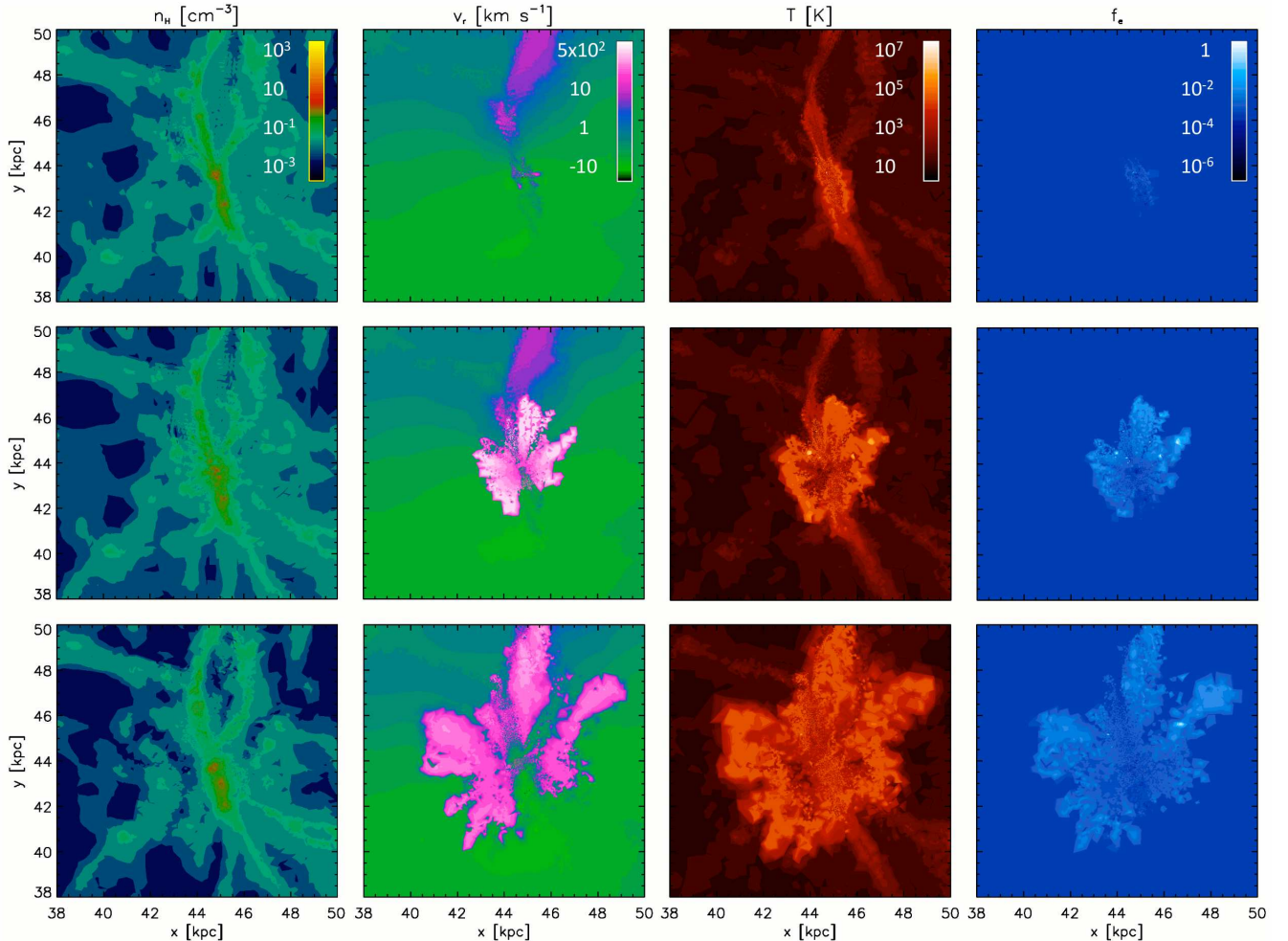


FIG. 4.— Properties of the gas in the vicinity of the SN at 1 Myr (*top panels*), 10 Myr (*middle panels*) and 50 Myr (*bottom panels*) after the explosion. From left to right, are projections of the number density of hydrogen nuclei, outward radial velocity, gas temperature and free electron fraction, within a 400 pc comoving slice around the explosion site. The lighter colors denote higher values for the quantities shown (see also Fig. 2). The explosion is asymmetric, with the shock propagating more rapidly into the low-density voids, instead of into the high-density filaments, of the cosmological density field (see also Fig. 7). While much of the swept-up mass is still outgoing at large velocities even after 50 Myr (*pink and white*), at this time metal-enriched gas is beginning to recollapse into the host halo where it will likely form second-generation stars (see Fig. 6).

a large fraction of the ejecta from our SMS SN consists of heavy elements. In particular, $\simeq 23,000 M_{\odot}$ of newly-synthesized metals are ejected in the explosion. These heavy elements are mixed with the primordial gas, enriching it to relatively high metallicity.

Figure 5 shows the average metallicity to which the gas in the vicinity of the explosion site is enriched by the ejecta, after 1 Myr, 10 Myr and 70 Myr. As the blast wave propagates outward into the low-density IGM gas at greater and greater radii becomes enriched. As metals are carried out of the host halo, metallicities at the smallest radii fall. After 70 Myr, however, the average metallicity of the gas out to almost 10 kpc (physical) is enriched to of the order of $10^{-2} Z_{\odot}$, and the densest gas which is recollapsing into the host halo is enriched to $\simeq 0.05 Z_{\odot}$. As shown in Figure 6, by 70 Myr the gas at the center of the SN remnant, shown in Figure 7, has recollapsed to densities of $n \sim 10^2 \text{ cm}^{-3}$, significantly more dense than the highest-density ($n \simeq 10 \text{ cm}^{-3}$) gas that remained within the virial radius of the host halo

~ 10 Myr after the SN. Not only is the gas recollapsing after 70 Myr, but, as shown in the right panel of Fig. 6, a portion of the SN ejecta is entrained in this gas. If this ejecta is well-mixed with the dense primordial gas, then we expect its metallicity to be $\simeq 0.05 Z_{\odot}$, as indicated in Fig. 5.

Gas enriched to such a high metallicity is predicted to readily fragment into low-mass stars (e.g., Bromm et al. 2001; Santoro & Shull 2006; Schneider et al. 2006), even in the presence of the elevated LW background radiation field expected in regions of the universe where SMSs form (e.g., Omukai et al. 2008). Therefore, we expect that second-generation stars would form from this SMS SN-enriched gas, and that a large fraction of these would have masses low enough ($\lesssim 0.8 M_{\odot}$) that they could still be present in the Galaxy today. While the nucleosynthetic signature of very massive Pop III pair-instability SNe (i.e., $140\text{--}260 M_{\odot}$) has yet to be uncovered in extremely metal-poor stars (Cayrel et al. 2004; Beers & Christlieb 2005; Frebel et al 2005; Lai et al 2008; Joggerst

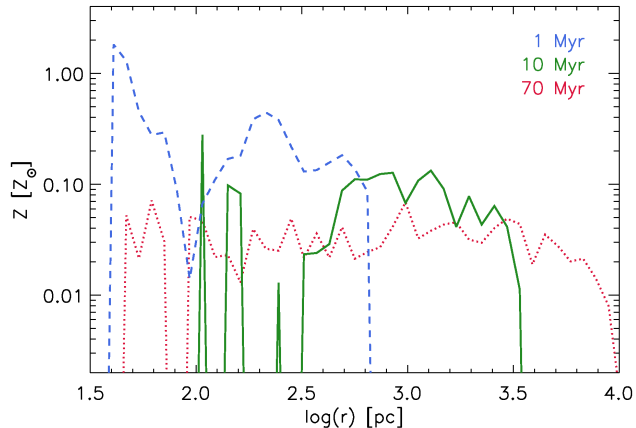


FIG. 5.— The spherically-averaged metallicity, Z , of the gas (in units of the solar metallicity Z_{\odot}), as a function of distance r from the explosion site, at 1 Myr (blue dashed line), 10 Myr (green solid line) and 70 Myr (red dotted line). As the metal-enriched gas is blown out of the halo, the metallicity in the interior region drops rapidly, while the IGM (outside the $\approx 10^3$ pc virial radius of the host halo) is enriched with metals out to continually larger radii. After 70 Myr, the gas recollapsing into the host halo (see also Fig. 6) has a metallicity of $\approx 0.05 Z_{\odot}$.

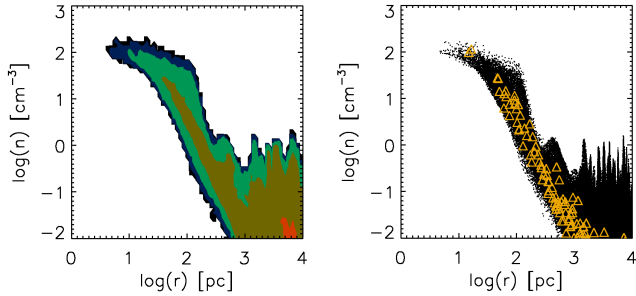


FIG. 6.— The hydrogen nuclei number density n , as a function of the distance r from the explosion site, at 70 Myr after the SN. As in Fig. 2, the contours in the left panel denote the distribution of the gas, the mass fraction varying by an order of magnitude across contour lines. Individual SPH particles are shown in the right panel, with those constituting the metal-rich SN ejecta denoted by orange triangles, as in Fig. 1. The highest-density gas is recollapsing into the halo which hosted the SN, where it will likely form second-generation stars. While the majority of the metal-rich ejecta particles are in the low density intergalactic medium, the densest gas comprises some of them, suggesting that the second-generation stars will be highly metal-enriched. Many such stars would likely be long-lived and could still exhibit the chemical signature of SMS SNe today.

et al 2010; Joggerst & Whalen 2011), it may have been found in high-redshift damped Lyman alpha absorbers (Cooke et al. 2011), and a number of metal-poor stars in a recent extension to the SEGUE survey have now been selected for spectroscopic followup on suspicion that they too may harbor this pattern (Ren et al. 2012). Furthermore, most stars forming in the ashes of very massive primordial SNe were likely enriched to metallicities above those targeted by surveys of metal-poor stars to date (Karlsson et al. 2008), and our simulations predict that second-generation stars formed from gas enriched by SMS SNe will have metallicities above $10^{-2} Z_{\odot}$, which are also above this threshold. We conclude that, while SMS SNe are almost certainly rare events, their chemical

signature might well be found in some of the ancient but not very metal-poor stars inhabiting our Galaxy today.

4. DISCUSSION AND CONCLUSIONS

We have carried out a multi-scale simulation of the explosion of a $55,000 M_{\odot}$ SMS, which, with an energy approaching 10^{55} erg, is among the biggest explosions in the history of the universe. With our multi-code approach, we have captured self-consistently, and for the first time, the essential radiation hydrodynamic features of the explosion at early times and the interaction of the blast wave with its host protogalaxy and with the IGM at later times.

Although the atomic cooling halos expected to host the formation of SMSs are at least two orders of magnitude more massive than the DM halos in which the first primordial stars are expected to form, we have found that these SMS SNe are energetic enough to completely evacuate them of dense gas. The metal-enriched ejecta is dispersed well beyond the ~ 1 kpc virial radius of the host halo, out to ~ 5 – 10 kpc into the low-density IGM, after ~ 50 Myr. By this time, $\sim 99\%$ of the kinetic energy in the explosion has been radiated away; nonetheless, the expansion of the shock into the IGM continues even at these late times, as the remaining kinetic energy is still comparable to that expected for a $\sim 200 M_{\odot}$ Pop III PSN.

Because of the deep potential well of the halo and ongoing accretion from filaments, after 70 Myr a fraction of the metal-enriched gas in the SN remnant, shown in Fig. 7, has recollapsing to high densities. Given the relatively high metallicity of this gas ($\sim 0.05 Z_{\odot}$),⁵ it is most likely that it will fragment vigorously and form a cluster of second-generation stars. Enriched to this metallicity, any of these stars which survive to the present-day would exhibit metallicities much higher than the most metal-poor stars that have been found in surveys of the Galactic halo. Indeed, although SMS SN are likely rare events, it is possible that their chemical signature could be found in very old, relatively high-metallicity Pop II stars which inhabit the Milky Way today (or in present-day dwarf galaxies; Frebel & Bromm 2012). As we expect SMS SNe to produce very little ^{56}Ni (Heger et al. 2013), their chemical signature may be distinguishable from those of most very massive (i.e., 140 – $260 M_{\odot}$) Pop III explosions (PSNe), which can produce iron-group elements (Heger & Woosley 2002). Similar to these PSNe, however, SMS SNe would not make any s -process or r -process contributions.

Finding the chemical signature of SMS SNe in low-mass, long-lived stars (or in the IGM; see e.g., Cooke et al. 2011) would be one way of verifying that such exotic events occurred in the early universe. Another possibility is that these gargantuan explosions could be found in

⁵ Previous cosmological simulations of metal enrichment by massive Pop III stars have shown second-generation star-forming gas to have typical metallicities of $\gtrsim 10^{-3} Z_{\odot}$ (e.g., Wise & Abel 2008; Greif et al. 2010; Ritter et al. 2012; Vasiliev et al. 2012; see also Wise et al. 2012; Safranek-Shrader et al. 2013). Incidentally, we note that Greif et al. (2007) arrived at comparable results by tracking metal enrichment using a much smaller number of SPH particles than we have used to track it here. Thus, we expect that our results with regard to metal enrichment should be broadly consistent with what would be found using other approaches.

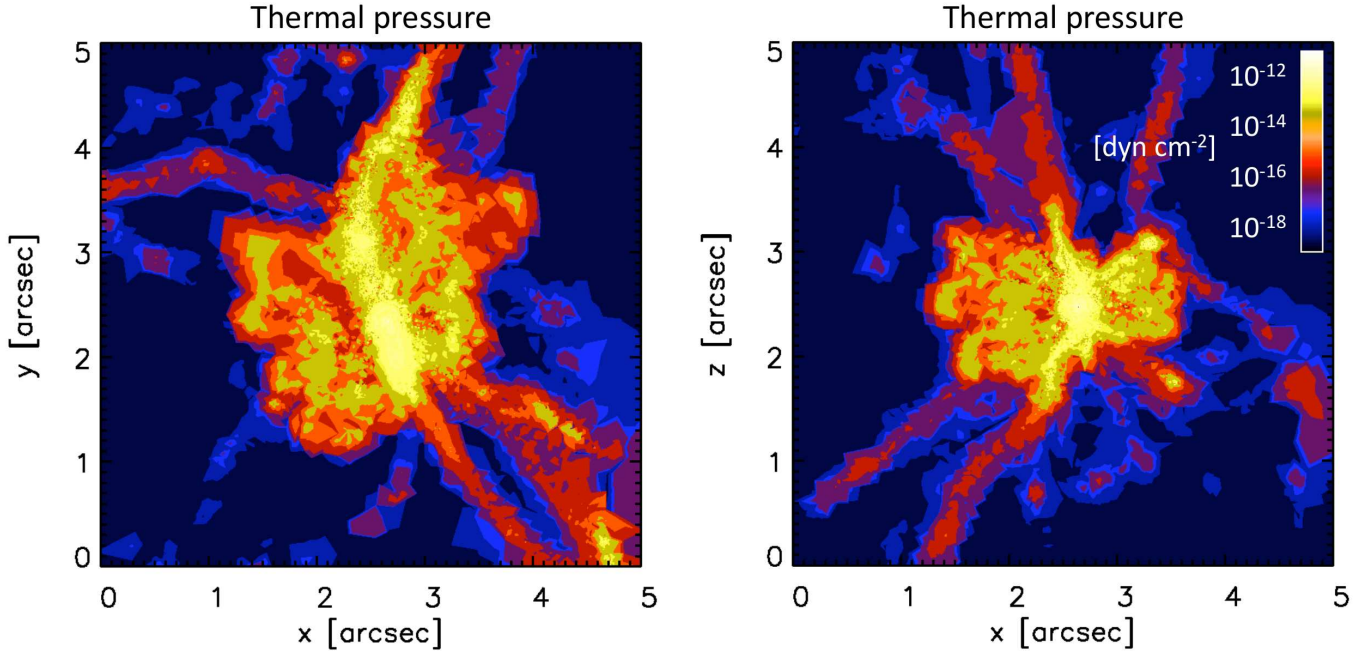


FIG. 7.— The SMS SN remnant 70 Myr after the explosion (at $z \simeq 13$), as seen on the sky from two orthogonal viewing angles, with colors corresponding to the thermal pressure of the gas as shown. Due to the inhomogeneous cosmological density field into which the blast wave propagates, the remnant takes on an irregular shape which can subtend up to ~ 3 arcsec, making it many times larger than most galaxies at this early epoch. Indeed, it is likely that such remnants could envelop entire early star-forming galaxies (see Section 4). SMS SNe may be detected in all-sky surveys, such as those planned for WFIRST and WISH. At the center of this remnant, a cluster of metal-enriched second-generation stars is expected to form (see Fig. 6).

all-sky surveys such as those planned for the *Wide-field Infrared Survey Telescope* (WFIRST) and the *Wide-field Imaging Surveyor for High-redshift* (WISH), as shown recently by Whalen et al. (2012a).⁶ Given that SMSs are expected to form in regions subjected to a large flux of LW radiation from nearby (within ~ 10 kpc; Dijkstra et al. 2008; Agarwal et al. 2012) star-forming galaxies, detection of SMS SNe would pinpoint locations on the sky where rapidly-forming first galaxies could be found in follow-up observations by the *James Webb Space Telescope*. Indeed, these explosions are so large that the SN remnants they leave behind, as shown in Fig. 7, are likely to be many times larger than, and in fact are likely to envelop, any such neighboring star-forming galaxies.

Could later stages of SMS SNe be detected by other means? They might appear in the radio at 21 cm. Meiksin & Whalen (2013) recently found that synchrotron emission from hypernovae in relatively dense media will be visible at 21 cm to existing radio facilities such as eVLA and eMERLIN in addition to the *Square Kilometer Array* (SKA). With their much higher energies and similar circumstellar densities, SMS SNe may be much brighter in the radio and detectable in all-sky surveys in spite of their small numbers. We are now calculating the radio signatures of SMS SNe in $z \sim 15$ protogalaxies.

Likewise, Oh et al. (2003) and Whalen et al. (2008) examined the potential imprint of Pop III SNe on the cosmic microwave background (CMB) via the Sunyaev-Zeldovich (SZ) effect. They found that a population of

140–260 M_{\odot} PSNe might impose excess power on the CMB on small scales, but with two caveats. First, the explosions must occur in large H II regions because the SN shock must still be hot by the time it encloses a large volume of CMB photons. Explosions in dense media dissipate too much heat to have an appreciable SZ signature or upscatter many CMB photons. Second, although a population of Pop III SNe might collectively impose features on the CMB individual remnants achieve radii just below the current resolution of *Atacama Cosmology Telescope* or the *South Pole Telescope*. Our models explode in dense environments and at redshifts at which inverse Compton cooling losses are lower than for the first SNe, but they eventually reach radii that would allow them to be resolved by current instruments. We are currently evaluating the SZ signatures of SMS SNe.

ACKNOWLEDGEMENTS

This work was supported by the U.S. Department of Energy through the LANL/LDRD Program, and JLJ acknowledges the support of a LDRD Director’s Postdoctoral Fellowship at Los Alamos National Laboratory. The RAGE and GADGET simulations were carried out on the LANL Institutional Computing clusters Pinto and Mustang, respectively. DJW acknowledges support from the Baden-Württemberg-Stiftung by contract research via the programme Internationale Spitzenforschung II (grant P- LS-SPII/18). AH and KC were supported by the US DOE Program for Scientific Discovery through Advanced Computing (SciDAC; DE-FC02-09ER41618), by the US Department of Energy under grant DE-FG02-87ER40328, by the Joint Institute for Nuclear Astrophysics (JINA; NSF grant PHY08-22648

⁶ We note that neutrino emission from these explosions (produced as discussed in e.g., Kistler & Beacom 2006; Yamazaki 2009; Morlino et al. 2009; Yuan et al. 2010) might also be detectable.

and PHY110-2511). AH acknowledges support by an ARC Future Fellowship (FT120100363) and a Monash University Larkins Fellowship. KC was supported by a KITP/UCSB Graduate Fellowship and by a UMN Stanwood Johnston Fellowship. The authors thank Avery

Meiksin for helpful discussion. Work at LANL was done under the auspices of the National Nuclear Security Administration of the U.S. Department of Energy at Los Alamos National Laboratory under Contract No. DE-AC52-06NA25396.

REFERENCES

- Abel, T., Bryan, G. L., Norman, M. L. 2002, *Sci*, 295, 93
 Almgren, A. S., et al. 2010, *ApJ*, 715, 1221
 Agarwal, B., Khochfar, S., Johnson, J. L., Neistein, E., Dalla Vecchia, C., Livio, M. 2012, *MNRAS*, 425, 2854
 Agarwal, B., Davis, A. J., Khochfar, S., Natarajan, P., Dunlop, J. S. 2013, *MNRAS*, submitted (arXiv:1302.6996)
 Alvarez, M. A., Wise, J. H., Abel, T. 2009, *ApJ*, 701, L133
 Appenzeller, I., Fricke, K. 1972, *A&A*, 21, 285
 Begelman M. C. 2010, *MNRAS*, 402, 673
 Begelman M. C., Volonteri M., Rees M. J. 2006, *MNRAS*, 370, 289
 Beers, T. C., Christlieb, N. 2005, *ARA&A*, 43, 531
 Bond, J. R., Arnett, W. D., Carr, B. J. 1984, *ApJ*, 280, 825
 Bromm, V., Ferrara, A., Coppi, P. S., Larson, R. B. 2001, *MNRAS*, 328, 969
 Bromm, V., Loeb, A. 2003, *ApJ*, 596, 34
 Bromm V., Larson R. B. 2004, *ARA&A*, 42, 79
 Cayrel, R., et al. 2004, *A&A*, 416, 1117
 Choi, J.-H., Shlosman, I., Begelman, M. C. 2013, *ApJ*, submitted (arXiv:1304.1369)
 Clark, P. C., Glover, S. C. O., Smith, R. J., Greif, T. H., Klessen, R. S., Bromm, V. 2011, *Sci*, 331, 1040
 Cooke, R., Pettini, M., Steidel, C. C., Rudie, G. C., Jogenson, R. A. 2011, *MNRAS*, 412, 1047
 de Souza, R. S., Rodrigues, L. F. S., Ishida, E. E. O., Opher, R. 2011, *MNRAS*, 415, 2969
 de Souza, R. S., Ishida, E. E. O., Johnson, J. L., Whalen, D. J., Mesinger, A. 2013, *MNRAS*, submitted (arXiv:1306.4984)
 Dijkstra, M., Haiman, Z., Mesinger, A., Wyithe, J. S. B. 2008, *MNRAS*, 391, 1961
 Fan, X., et al. 2006, *AJ*, 131, 1203
 Fowler, W. A., Hoyle, F. 1964, *ApJS*, 9, 201
 Frebel, A., et al. 2005, *Nat*, 434, 871
 Frebel, A., Bromm, V. 2012, *ApJ*, 759, 115
 Frey, L., Even, W., Whalen, D. J., et al. 2013, *ApJS*, 204, 16
 Fryer, C. L., Heger, A. 2011, *AN*, 332, 408
 Fuller, G. M., Woosley, S. E., Weaver, T. A. 1986, *ApJ*, 307, 675
 Fuller, G. M., Shi, X. 1998, *ApJ*, 502, L5
 Gittings, M., et al. 2008, *CS&D*, 1, 5005
 Greif T. H., Johnson J. L., Bromm V., Klessen R. S. 2007, *ApJ*, 670, 1
 Greif T. H., Glover, S. C. O., Bromm, V., Klessen, R. S. 2010, *ApJ*, 716, 510
 Greif T. H., Springel, V., White, S. D. M., Glover, S. C. O., Clark, P. C., Smith, R. J., Klessen, R. S., Bromm, V. 2011, *ApJ*, 737, 75
 Heger, A., Woosley, S. E. 2002, *ApJ*, 567, 532
 Heger, A., et al. 2013, in prep
 Hosokawa, T., Omukai, K., Yorke, H. W. 2012, *ApJ*, submitted (arXiv:1203.2613)
 Hummel, J. A., Pawlik, A. H., Milosavljević, M., Bromm, V. 2012, *ApJ*, 755, 72
 Iben, I. 1963, *ApJ*, 138, 1090
 Inayoshi, K., Omukai, K. 2012, *MNRAS*, 422, 2539
 Inayoshi, K., Hosokawa, T., Omukai, K. 2013, *MNRAS*, accepted (arXiv:1302.6065)
 Jeon, M., Pawlik, A. H., Greif, T. H., Glover, S. C. O., Bromm, V., Milosavljević, M., Klessen, R. S. 2012, *ApJ*, 754, 34
 Joggerst, C. C., Whalen, D. J. 2011, *ApJ*, 728, 129
 Joggerst, C. C., Almgren, A., Bell, J., Heger, A., Whalen, D. J., Woosley, S. E. 2010, *ApJ*, 709, 11
 Johnson, J. L., Dalla Vecchia, C., Khochfar, S. 2013, *MNRAS*, 428, 1857
 Johnson, J. L., Khochfar, S., Greif, T. H., Durier, F. 2011, *MNRAS*, 410, 919
 Johnson, J. L., Whalen, D. J., Fryer, C. L., Li, H. 2012b, *ApJ*, 750, 66
 Johnson, J. L., Whalen, D. J., Li, H., Holz, D. E. 2012a, *ApJ*, submitted (arXiv:1211.0548)
 Karlsson, T., Johnson, J. L., Bromm, V. 2008, *ApJ*, 679, 6
 Kistler, M. D., Beacom, J. F. 2006, *PhRvD*, 74, 063007
 Kitayama T., Yoshida N. 2005, *ApJ*, 630, 675
 Komatsu, E., et al. 2011, *ApJS*, 192, 18
 Lai, D. K., Bolte, M., Johnson, J. A., Lucatello, S., Heger, A., Woosley, S. E. 2008, *ApJ*, 681, 1524
 Latif, M. A., Schleicher, D. R. G., Schmidt, W., Niemeyer, J. 2013a, *MNRAS*, 430, 588
 Latif, M. A., Schleicher, D. R. G., Schmidt, W., Niemeyer, J. 2013b, *MNRAS*, submitted (arXiv:1304.0962)
 Linke, F., Font, J. A., Janka, H.-T., Müller, E., Papadopoulos, P. 2001, *A&A*, 376, 568
 Lodato, G., Natarajan, P. 2006, *MNRAS*, 371, 1813
 McKee, C. F., Tan, J. C. 2008, *ApJ*, 681, 771
 Meiksin, A., Whalen, D. J. 2013, *MNRAS*, 430, 2854
 Milosavljević, M., Bromm, V., Couch, S. M., Oh, S. P. 2009, *ApJ*, 698, 766
 Montero, P. J., Janka, H.-T., Müller, E. 2012, *ApJ*, 749, 37
 Morlino, G., Blasi, P., Amato, E. 2009, *Astropart. Phys.*, 31, 376
 Mortlock, D. J., et al. 2011, *Nat*, 474, 616
 Natarajan, P., Volonteri, M. 2012, *MNRAS*, 422, 2051
 Oh, S. P., Cooray, A., Kamionkowski, M. 2003, *MNRAS*, 342, L20
 Omukai, K., Schneider, R., Haiman, Z. 2008, *ApJ*, 686, 801
 O’Shea B. W., Norman M. L. 2008, *ApJ*, 673, 14
 Pan, T., Kasen, D., Loeb, A. 2012, *MNRAS*, 422, 2701
 Park, K., Ricotti, M. 2012, *ApJ*, 747, 9
 Peluupessy, F. I., Di Matteo, T., Ciardi, B. 2007, *ApJ*, 665, 107–119
 Petri, A., Ferrara, A., Salvaterra, R. 2012, *MNRAS*, accepted (arXiv:1202.3141)
 Planck Collaboration, A&A submitted (arXiv:1303.5076)
 Regan J. A., Haehnelt M. G. 2009, *MNRAS*, 396, 343
 Ren, J., Christlieb, N., Zhao, G. 2012, *RAA*, 12, 1637
 Ritter, J. S., Safranek-Shrader, C., Gnat, O., Milosavljević, M., Bromm, V. 2012, *ApJ*, 761, 56
 Safranek-Shrader, C., Milosavljević, M., Bromm, V. 2013, *MNRAS*, submitted (arXiv:1307.1982)
 Santoro, F., Shull, J. M. 2006, *ApJ*, 643, 26
 Scannapieco, E., Madau, P., Woosley, S., Heger, A., Ferrara, A. 2005, *ApJ*, 633, 1031
 Schleicher, D. R. G., Palla, F., Ferrara, A., Galli, D., Latif, M. 2013, *A&A*, submitted (arXiv:1305.5923)
 Schneider, R., Omukai, K., Inoue, A. K., Ferrara, A. 2006, *MNRAS*, 369, 825
 Sethi, S., Haiman, Z., Pandey, K. 2010, *ApJ*, 721, 615
 Shang, C., Bryan, G. L., Haiman, Z. 2010, *MNRAS*, 402, 1249
 Shapiro, S. L. 2005, *ApJ*, 620, 59
 Shapiro, S. L., Teukolsky, S. A. 1979, *ApJ*, 234, L177
 Smith, R. J., Glover, S. C. O., Clark, P. C., Greif, T. H., Klessen, R. S. 2011, *MNRAS*, 414, 3633
 Spaans, M., Silk, J. 2006, *ApJ*, 652, 902
 Springel V., Yoshida N., White S. D. M., 2001, *NewA*, 6, 79
 Springel V., Hernquist, L. 2002, *MNRAS*, 333, 649
 Tanaka, M., Moriya, T. J., Yoshida, N., Nomoto, K. 2012, *MNRAS*, 422, 2675
 Tanaka, M., Moriya, T. J., Yoshida, N. 2013, *MNRAS*, submitted (arXiv:1306.3743)
 Van Borm, C., Spaans, M. 2013, *A&A*, submitted (arXiv:1304.4057)
 Vasiliev, E. O., Vorobyov, E. I., Matvienko, E. E., Razoumov, A. O., Shchekinov, Y. A. 2012, *ARep*, 56, 895
 Volonteri, M., Rees, M. 2006, *ApJ*, 650, 669
 Volonteri, M. 2012, *Sci*, 337, 544
 Volonteri, M., Begelman, M. C. 2010, *MNRAS*, 409, 1022
 Vorobyov, E. I., DeSouza, A. L., Basu, S. 2013, *ApJ*, submitted (arXiv:1303.3622)
 Weaver, T. A., Zimmerman, G. B., Woosley, S. E. 1978, *ApJ*, 225, 1021
 Whalen D., van Veelen B., O’Shea B. W., Norman M. L. 2008, *ApJ*, 682, 49
 Whalen, D. J., Heger, A., Chen, K.-J., Even, W., Fryer, C. L., Stiavelli, M., Xu, H., Joggerst, C. C. 2012a, *ApJ*, submitted (arXiv:1211.1815)
 Whalen, D. J., Abel, T., Norman, M. L. 2004, *ApJ*, 610, 14
 Whalen, D. J., et al. 2013a, *ApJ*, 768, 195
 Whalen, D. J., et al. 2012b, *ApJ*, submitted (arXiv:1211.4979)
 Whalen, D. J., et al. 2013b, *ApJ*, 768, 95
 Whalen, D. J., et al. 2013c, *ApJL*, 762, 6
 Whalen, D. J., et al. 2013d, *ApJ*, accepted (arXiv:1305.6966)
 Willott, C. J., McLure, R. J., Jarvis, M. J., 2003, *ApJ*, 587, L15
 Wise, J. H., Abel, T. 2007, *ApJ*, 671, 1559
 Wise, J. H., Turk, M. J., Abel, T. 2008, *ApJ*, 682, 745
 Wise, J. H., Abel, T. 2008, *ApJ*, 685, 40
 Wise, J. H., Turk, M. J., Norman, M. L., Abel, T. 2012, *ApJ*, 745, 50

Wolcott-Green, J., Haiman, Z., Bryan, G. L. 2011, MNRAS, 418,
838
Woosley, S. E., Heger, A., Weaver, T. A. 2002, RevMP, 74, 1015

Yamazaki, R., Kohri, K., Katagiri, H. 2009, A&A, 495, 9
Yoshida, N., Omukai, K., Hernquist, L. 2008, Sci, 321, 669
Yuan, Q., Yin, P., Bi, X. 2010, arXiv:1010.1901